

AD No. _____
DDC FILE COPY
406 929

406929

(4) \$2.60
(5) 749 200

63-4-1

(1)

(6) Mechanical Properties Of
Two-Phase Crystalline Materials

(7) MIT

(10) By
G. S. Ansell

(14) Technical Report No. 3

(11) 22 May, 1963

Office of Naval Research

(15) Contract NONR 591 (15)

(16) Project No. 031-689

Scale - 2

(12) 26 p.

(13) NA

(17) NA

(18) NA

(19) NA

(20) NA

NASA Interdisciplinary Materials Research Laboratory
Rensselaer Polytechnic Institute
Troy, New York

Reproduction in whole or in part is permitted for
any purpose of the United States Government

This paper is to be presented at the International
Symposium, High Temperature Technology

8-11 September 8-11, 1963,

Asilomar, California

DDC
RECEIVED
JUN 20 1963
TISIA A

\$2.60

17

MECHANICAL PROPERTIES OF TWO-PHASE CRYSTALLINE MATERIALS

By

G. S. Ansell

Associate Professor of Metallurgical Engineering
Rensselaer Polytechnic Institute
Troy, New York

Introduction

One method of enhancing the mechanical properties of a crystalline solid is by the addition of a distributed second-phase. In general, when a finely divided second-phase is distributed in a crystalline matrix, an alloy is formed which is considerably stronger than the single-phase matrix alone. These alloys are termed dispersion-strengthened alloys.

Although dispersion-strengthening is but one of several methods which may be utilized to increase the strength of a crystalline solid, it has assumed a predominant position in the consideration of strengthening solids for high temperature service applications.¹ This predominance arose largely due to the discovery by Irmann² that aluminum alloys produced by compacting, hot pressing, and extruding flake or atomized aluminum powders, possess remarkable high temperature properties including the retention of usable mechanical strength at temperatures as high as the melting point of aluminum. These SAP alloys consist of a dispersion of aluminum oxide particles in an aluminum matrix. During the powder consolidation process, the aluminum oxide coating originally present on each powder particle fractures and is dispersed within the alloy.

During the past 15 years since Irmann's discovery of the aluminum-aluminum oxide SAP alloys, a great deal of effort¹ has been expended to develop SAP-Type alloys, utilizing higher melting temperature elements for the matrix, in the hope that these dispersion-strengthened alloys would retain significant levels of strength at temperatures as close to the melting temperatures of these matrix elements as for the case of the aluminum-aluminum oxide SAP alloys. The successful development of these SAP-Type alloys has, however, not kept pace with this considerable effort.

To this date, not one high melting temperature matrix element dispersion-strengthened alloy has been developed which retains significant mechanical strength at comparable temperatures relative to the matrix melting temperature as the useful service temperatures of the SAP alloys. This unsuccessful developmental effort is symptomatic of the lack of fundamental knowledge concerning the nature of dispersion-strengthening.

(It is the purpose of this paper to present a theoretical approach to account for the observed strengthening behavior of dispersion-strengthened

alloys. Since the field of dispersion-strengthening is neither new nor sterile, it is necessary first to put this approach into some historical perspective.

That a dispersed second-phase strengthens a crystalline matrix, has long been recognized and made use of. Most of the commercially important engineering metal alloys derive their strengths on this basis. Well-known examples include steels containing dispersions of cementite in a ferrite matrix, be they in the form of lamellar cementite in a pearlitic structure, or of spheroidal cementite in a tempered martensitic structure. Precipitation-hardened ferrous and nonferrous alloys demonstrate a marked strengthening effect due to the finely dispersed precipitate phase. Historically, the metallurgist, although in the forefront amongst materials area disciplines in the use of the structure-properties correlation concept, strove to explain the observed strengthening of two-phase alloy systems, not upon the structural similarities generally common to these alloys, but instead, compartmentalized his thought within the framework of the processing which produced the structure. Hence, one finds precipitation hardening, dispersion-strengthening, and the hardening of steels explained both thoroughly and uniquely, but separately and inconsistently although each achieves its strength due to the presence of a finely distributed second-phase. Although of course the structures of these materials are obtained by different techniques, all have the same basic structure. Any mechanism proposed to account for the observed strengthening behavior of two-phase alloys must be applicable to all materials with similar structure independent of the method utilized to produce the structure.

Recent techniques, particularly transmission electron microscopy, have enabled the experimentalist to extend his view beyond observations of the microstructure and gross properties of crystalline materials to the deformation process itself. Any mechanism proposed to account for strengthening behavior must therefore not only predict the gross mechanical behavior of the material from knowledge of its structure, but also must be consistent with valid observations of the deformation process.

It is within this context that this paper has been written. The paper is not intended, however, to be a review of all work which has been performed in the field of dispersion-strengthening. Rather, an approach is presented which is proposed to account for the observed strengthening behavior of two-phase crystalline solids. Some aspects of this material have been published previously; others have not. In addition, many of the ideas included are of course controversial and should be considered as part of a continuing research program instead of the result of completed work.

General Approach

The theoretical treatment of the observed strengthening behavior of dispersion-strengthened alloys would be relatively easy if all the mechanical properties could be explained by one mechanism or calculation. Unfortunately, this is not possible. Any mechanical property involving plasticity has to be evaluated in terms of dislocation motion. However, the mode of dislocation motion responsible for one particular property may not be important for another property, e.g., at low temperatures one is not concerned with dislocation climb, whereas at high temperatures climb is necessary to explain recovery. Therefore, it is not possible to derive a unique theory which will explain all the mechanical properties of dispersion-strengthened alloys, but rather, each mechanical property must be treated individually.

1. Yield Strength Behavior

Plastic deformation in crystalline solids is due to the movement of dislocations. Crystals yield when large numbers of dislocations can move appreciable distances through the lattice. This process requires that under the action of an applied stress, two consecutive processes must occur: first, dislocations are generated at some source; and second, these dislocations move appreciable distances through the crystal. Whichever of these requires the higher stress - dislocation generation or dislocation mobility - controls the yielding behavior of the solid. In single-phase materials, either of these two processes may be controlling. In pure annealed metals, dislocation generation generally controls the yielding behavior. In solid solution strengthened metals and in some non-metallic crystals, dislocation mobility may be more restrictive.

In dispersion-strengthened alloys, however, the stress necessary to move dislocations appreciable distances along a lattice plane is higher than the stress required to generate dislocations from a source. In this case, the interaction of the dislocations with the dispersed second-phase particles controls dislocation mobility and hence the yielding behavior. Ansell and Lenel³ have proposed a model to account for the yielding behavior of dispersion-strengthened alloys. This model was later extended for the case of very fine dispersed-phase particles by Ansell.⁴

a) Model

Dislocations are formed at dislocation sources under the action of an applied stress. The nature of the sources is not critical in considering the model. As the dislocations expand from sources, they are either blocked from further motion by the second-phase particles, or they continue to move by bowing about the dispersed particles, leaving residual dislocation loops surrounding each particle. In either event, if the dislocation is completely blocked by the particles, or if the dislocations bow past the particles, yielding does not result. This postulate can be supported by the following simple argument:

The first dislocation generated at a source moves in the slip plane until it is blocked from further movement either by the dispersed particles, or by its interaction with dislocations nucleated from other sources. In single-phase materials this blockage of the lead dislocation by dislocations from other sources is overcome by the increase of stress on the dislocation due to the pile-up of subsequently nucleated dislocations behind the lead dislocation. In a dispersion-strengthened alloy, however, the lead dislocation remains blocked because: 1) the stress field of the residual loops decreases the effective stress on the dislocation source. Therefore, because the effective stress on the dislocation source is reduced, fewer dislocations are nucleated at each source; 2) the stress field of the residual loops interacts with the piled-up dislocation group, changing the pile-up spacing. This reduces the stress field ahead of the leading dislocation of the piled-up group of dislocations. Both of these factors decrease the stress on the lead dislocation, making it easier to be blocked. Therefore, the plastic strain, ϵ , of the dispersion-strengthened alloy is

$$\epsilon = M N \pi R^2 b \quad (1)$$

where \underline{M} is the density of the dislocation sources, \underline{N} is the number of dislocations nucleated at each source, \underline{R} is the average radius of the dislocation loops, and b is the Burgers vector of the dislocation. Assuming reasonable values for these, $\underline{M} = 10^9$ sources/cm³; $\underline{N} = 10$ dislocations/source; $\underline{R} = 1/2 (\underline{M}^{-1/3})$, and $b = 2 \times 10^{-8}$ cm., the resultant strain associated with yielding; e.g., the strain associated with the engineering offset yield stress is 2×10^{-3} . Therefore, plastic deformation stops, and yielding has not occurred when the back stress on the dislocation source, due to an array of either blocked dislocations or of residual loops around the particles, exceeds the applied stress. The choice of the value for the source density in the evaluation of equation (1) is not critical since the strain varies as the cube root of the source density. Under these conditions, in alloys with fine dispersions, no apparent yielding has yet occurred. In order to cause such yielding, the shear stress due either to the dislocations piled up against or around the particles much fracture or shear the dispersed second-phase particles. This fracturing or shearing of the dispersed particles relieves the back stress on the dislocation source, and also increases the stress on the lead dislocation. The dislocations then can sweep out areas on the slip plane which are large with respect to the dispersion spacing.

Even at one half or more of the absolute melting temperature of the matrix metal, fracture or shear of the second-phase particles should be necessary for appreciable yielding to occur unless recovery takes place. Recovery can occur either by climb of piled-up dislocations at a rate exceeding the applied strain rate, or by cross slip of piled-up dislocations out of the slip plane if the geometry of the dispersed phase particles permits. The possibility of recovery is not considered in the following calculations:

b) Calculations Based Upon Model.

On the basis of the preceding model, the yield strength of a dispersion-strengthened alloy is now evaluated. ^{3,4}

The method of calculation is straight forward. First the shear stress, τ , on the dispersed phase particle, due either to the lead dislocation from the dislocation source or to the inner residual dislocation loop if the lead dislocation has bowed past the dispersed particle, is calculated as a function of the externally applied stress on the crystal, σ . Then the shear stress, F , required to either shear or fracture the dispersed particle is evaluated. From these calculations, the yield stress of the dispersion-strengthened alloy or the externally applied stress required to shear or deform the dispersed particles, is determined.

The shear stress, τ , on the dispersed phase particle is:

$$\tau = n\sigma \quad (2a)$$

where n is the number of dislocations piled up against or looped around the dispersed particle, if the radius of curvature of the dislocation nearest the particle is greater than $\mu b/\sigma$, where μ is a shear modulus of the matrix crystal ($\mu = [\frac{1}{2} C_{44}(C_{11} - C_{12})]^{1/2}$ for cubic crystals, C_{ij} being the usual elastic constants).

If the radius of curvature of the dislocation nearest the particle is

less than $\mu b/\sigma$, the shear stress, τ , on the dispersed-phase particle is:

$$\tau = n \mu b / r \quad (2b)$$
 where r is the radius of curvature of the dislocation nearest the dispersed particle.

The number of dislocations, n , in equations (2a) and (2b), acting on the particle depends upon the spacing between particles according to the relation:

$$n = 2 \lambda \sigma / \mu b \quad (3)$$

where λ is the spacing between dispersed-phase particles.

Combining equations (2a) and (3), the shear stress on relatively large dispersed-phase particles; i.e., in the case of spherical particles, particles whose diameter, d , is greater than $2\mu b/\sigma$, is:

$$\tau = 2 \lambda \sigma^2 / \mu b \quad (4a)$$

Combining equations (2b) and (3), the shear stress on relative fine dispersed-phase particles; i.e., in the case of spherical particles, particles whose diameter, d , is less than $2\mu b/\sigma$, is:

$$\tau = 2 \lambda \sigma / r \quad (4b)$$

The shear stress, F , that will either shear or fracture the dispersed phase particle is in general proportional to a shear modulus, μ^* , of the particle. Therefore:

$$F = \mu^* / C \quad (5)$$

where C is a constant of proportionality, which can theoretically be shown to be in the neighborhood of 30. For some types of dispersed particles, particularly in the case of the metastable phases or zones which appear as the result of the heat treatment of some precipitation hardened alloys, other methods⁶ of evaluating the shear strength, F , of the particles have been utilized. If a system is considered where such an alternative estimate of the shear strength appears warranted, its substitution for the shear strength predicted by equation (5) would be justified.

Combining equations (4a) and (5), the yield strength, $\sigma_{y.s.}$ of a dispersion-strengthened alloy containing relatively coarse dispersed-phase particles is:

$$\sigma_{y.s.} = (\mu b \mu^* / 2 \lambda C)^{1/2} \quad (6a)$$

Combining equations (4b) and (5), the yield strength, $\sigma_{y.s.}$ of a dispersion strengthened alloy containing fine dispersed-phase particles is:

$$\sigma_{y.s.} = \mu^* r / 2 \lambda C \quad (6b)$$

Since it can be shown that in the case of an alloy containing spherical particles that:

$$\frac{\lambda + d}{d} = \frac{0.82}{f^{1/3}} \quad (7)$$

where f is the volume fraction of second-phase particles, equation (6b) may be rewritten in the form:

$$\sigma_{y.s.} = \frac{\mu^*}{4C} \cdot 5^{1/3} \left(\frac{1}{0.82 - f^{1/3}} \right) \quad (8)$$

When the dispersed-phase particles are not spherical, it becomes necessary to judiciously evaluate the particle size which delineates the boundary between the use of the computations for either the relatively coarse or fine particles. The two computational treatments are of course

compatible with the model, each being the limiting case of the other.

c) Alloy Design Based Upon Yield Strength Calculations.

The design of two-phase materials as regards yielding behavior is discussed on the basis of the preceding calculations. Before entering into specific discussions of this area, however, it is necessary to consider the physical significance of the yield strength as calculated by use of equations (6a), (6b), and (8). This yield strength is the stress required to produce appreciable or measurable plastic deformation. As such, it is most closely identified with either the critical resolved shear stress of single crystals or the elastic limit of polycrystalline materials. In the case of polycrystalline materials, the engineering offset yield stress would be higher than, but proportional to, the calculated yield strength.

1) Materials Selection: The shear modulus is the only property of either the matrix or dispersed phase which affects the yielding behavior of two-phase materials. For two-phase materials where the dispersed particle's diameter is greater than $2\mu_b/\sigma_{y.s.}$, the yield strength is proportional to the square root of the product of the matrix and dispersed-phase shear moduli. For two-phase materials where the dispersed particle's diameter is less than $2\mu_b/\sigma_{y.s.}$, the yield strength is proportional to the shear modulus of the dispersed phase. In the design of two-phase materials for high yield strengths, therefore, a dispersed-phase with a high shear modulus should always be selected, while the shear modulus of the matrix is only important if the dispersed particle size is relatively large. This leads to the interesting conclusion, that if the dispersed-phase particle size is sufficiently fine, the yield strength of the two-phase material is independent of the choice of matrix phase.

11) Dispersed Phase Morphology. Consideration of equations (6a) and (6b) indicates that the finer the spacing between dispersed phase particles of constant size, the higher the yield strength of the two-phase material. For such materials, the yield strength is proportional to the reciprocal square root of the dispersion spacing for dispersed particles whose diameter is greater than $2\mu_b/\sigma_{y.s.}$ and is proportional to the reciprocal of the dispersion spacing for materials containing dispersed particles of finer size. These relationships are shown schematically in Figures 1 and 2. If, however, one considers the strength of a two-phase material containing a given volume fraction of dispersed phase, but varies the interparticle spacing by changing the particle size, this continued increase of yield strength with decreasing interparticle spacing no longer holds. As indicated by equations (6a) and (8), and as illustrated in Figure 3, for a two-phase material containing a constant volume fraction of a second phase, if the second phase is subdivided into finer and finer spherical particles, decreasing the interparticle spacing, the yield strength increases with the reciprocal square root of the dispersion spacing until the particle diameter is less than $2\mu_b/\sigma_{y.s.}$. For particle sizes smaller than this, the yield strength reaches a maximum limit roughly proportional to the cube root of the volume fraction of dispersed phase. In fabricating a two-phase material for highest yield strength, the matrix should contain the largest practical volume fraction of second phase particles whose maximum particle diameter is:

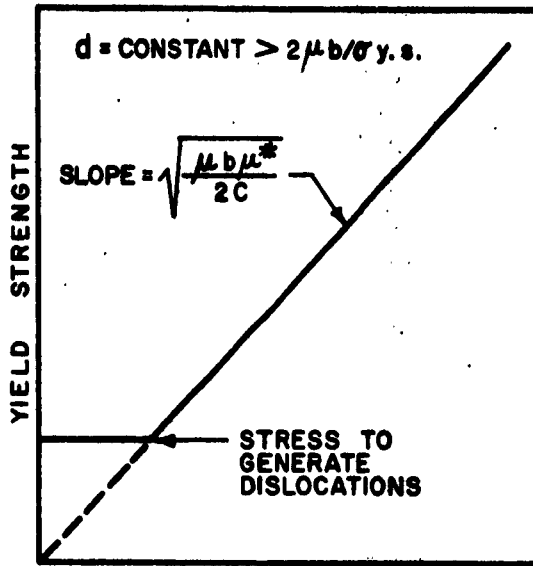


Figure 1: Schematic plot of yield strength as a function of the reciprocal square root of dispersion spacing for alloys containing large particles of constant diameter.

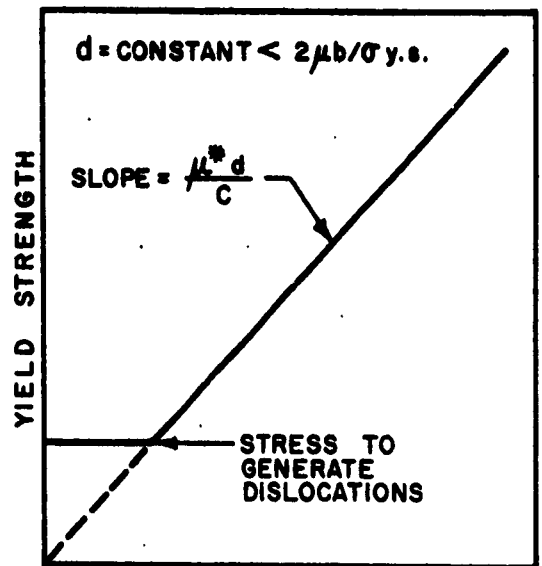


Figure 2: Schematic plot of yield strength as a function of the reciprocal of dispersion spacing for alloys containing fine particles of constant diameter.

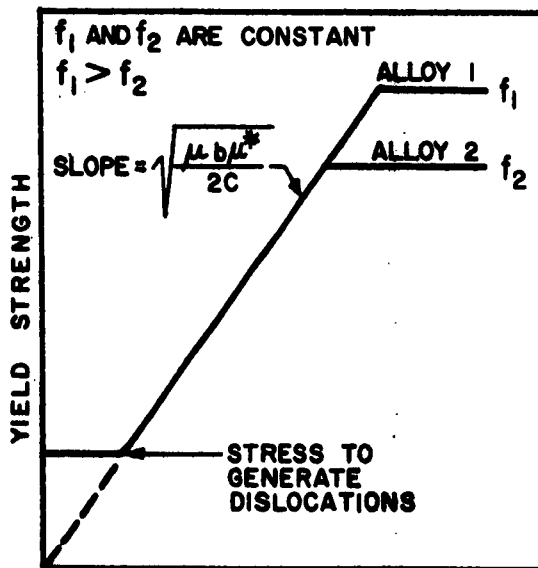


Figure 3: Schematic plot of yield strength as a function of the reciprocal square root of dispersion spacing for two alloys each containing a constant volume fraction of second phase.

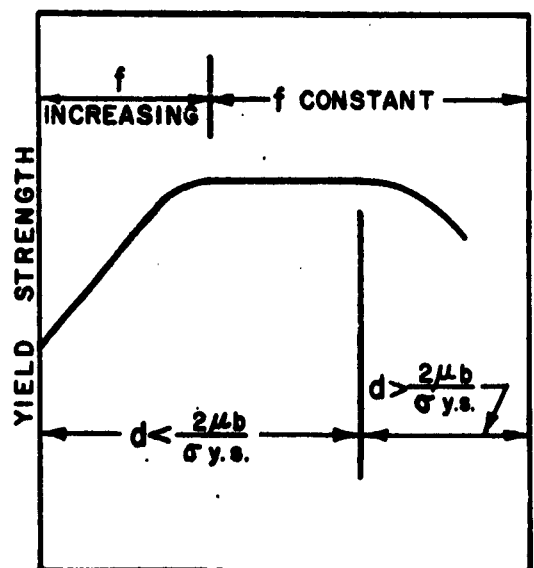


Figure 4: Schematic plot of yield strength as a function of aging time for a precipitation hardened alloy.

The effect of particle shape upon yielding behavior is important for two reasons. Firstly, if the dispersed phase is not spherical, it is difficult to determine the particle size below which the shear stress on the dispersed particle due to the radius of curvature of the dislocation next to the particle becomes important. Secondly, if the matrix system is such that recovery by cross slip can occur, then the particle size and spacing become very important. This is particularly evident in a matrix with a high stacking fault energy; e.g., aluminum. One can assume, however, that if the height of the dispersed phase is approximately twice the particle spacing, cross slip can be neglected. If the height of the particle is not this large, cross slip will probably occur in a high stacking fault energy matrix. For these latter alloys, dispersion strengthening can occur, but the yield strength will not be governed by the shear or fracture stress of the second phase particle, but rather by some function of the cross slip geometry,

iii) Dispersed Particle - Matrix Interface. In order to increase the yield strength of a crystalline matrix, the dispersed phase must impede the movement of dislocations. In order for the dispersed particles to hinder dislocation movement, the dislocations must be repelled from the dispersed phase-matrix interface. Therefore, the interface has to be of such a nature that in itself it is a barrier to dislocation motion, or that the strain field of the dislocation can be mechanically transmitted from the matrix lattice, through the interface, into the lattice of the dispersed phase. In order to accomplish this, the matrix has to either "wet", adhere to, or cohere with the dispersed phase particles. This characteristic of dislocation interaction through an interface, with another phase, has been clearly shown by Barrett¹ in his experimental investigations of the elastic after-effect for wires twisted in torsion. A similar investigation of the presence or absence of the elastic after-effect in wires of the matrix metal coated with a proposed dispersed phase should give good indication of whether the interface between the two phases of a particular two-phase system possesses this required property.

This discussion brings out the fact that in order to obtain dispersion strengthening, the second phase may cohere, but does not have to cohere to the matrix. The principal characteristic of the coherency effect is the lattice strain it produces in both the matrix and the second phase. If the coherency strain changes either the matrix modulus around the dispersed particle or the dispersed phase modulus, then it will affect the interaction between dislocations and the dispersed particle. For the purpose of calculating dispersion strengthening effects, the size of a complex consisting of the precipitated particle and the strained coherent region of the matrix surrounding it where the modulus is significantly changed should be important, rather than the size of the particle alone.

iv) Service Temperature. The effect of temperature upon the yielding behavior of dispersion-strengthened alloys is a two-fold one.

First, the yield strength of these alloys is directly dependent upon the dispersed phase particle size and distribution. Any change in the dispersed phase morphology of an alloy will, therefore, change its yield strength. For elevated service application, the major problem is therefore

structural stability. Any dispersed phase structure which is produced by a second-phase rejection from a solid solution is inherently unstable for service use at elevated temperatures. The degree of instability varies with both the system and the service temperature. Most precipitation hardened alloys, for example, maintain a stable dispersed phase structure at temperatures up to 100 to 200°C below the temperature at which the second phase was formed. In this temperature range the rate of second phase coarsening is slow enough to be considered negligible. For example, martensite tempered at 500°C would be suitable for service use at temperatures as high as 350°C. On the other hand, some of the nickel base superalloys make use of a complex precipitation structure to maintain a constant dispersed phase structure at very high temperatures. During high temperature service, precipitate particles are continuously rejected from solid solution to replace those particles which have coarsened. In these alloys, a dynamic structural equilibrium is maintained to insure useful service properties.

The ultimate in maximum possible service temperature of a dispersion-strengthened alloy is the melting point of the matrix metal. The aluminum-aluminum oxide "SAP-Type" alloys fall into this category. The aluminum oxide particles are completely stable in the aluminum matrix. In order to design other dispersion-strengthened alloys which also have this ultimate useful service temperature, the second phase must be produced by techniques other than by rejection from solid solution. Some techniques which can be used include: 1) consolidation of fine metal powders which are coated with a stable second-phase by powder metallurgical techniques;⁸ 2) consolidation of fine duplex phase metal powders in which one phase has been formed during powder production by rejection from the melt and is insoluble in the solid matrix; e.g., copper in lead;⁹ 3) consolidation of fine powder mixtures of the matrix and dispersed phases.¹⁰ In order to maintain the maximum structural stability, at least one component of the dispersed phase must be completely insoluble and non-diffusible in the matrix metal.

Second, if the structure is completely stable, the yield strength still shows some variation with temperature. This arises due to the change in the elastic constants of the alloy associated with temperature. Inspection of equations (6a) and (8) shows that of the terms which determine the yield strength of a dispersion-strengthened alloy only the shear moduli have an appreciable temperature dependence. Therefore, if the temperature dependence of these moduli is known, or if a reasonable approximation of this dependence can be made, the variation of the yield strength with temperature should be predictable.

It is interesting to consider the design of a two-phase material where the temperature dependence of the yield strength does not reflect the temperature dependence of the matrix phase. This is of particular importance for very high temperature applications, where the service temperature is high as compared to the melting temperature of the matrix. In this temperature range, the shear modulus of the matrix would decrease rapidly. If the dispersed phase particle size is less than $\frac{2\mu b}{\sigma_{y.s.}}$, the temperature dependence of the yield strength of the two-phase material is only dependent upon the temperature dependence of the shear modulus of the dispersed phase. This would dictate the selection of a dispersed phase which had a considerably higher melting temperature than the melting temperature of the matrix,

and a dispersed particle diameter less than $2\mu b/\sigma_{y.s.}$ when designing an alloy for high temperature service.

d) Consistency of Yielding Behavior Theory with Experimental Observations.

In order to consider the validity of this proposed treatment of the yielding behavior of two-phase crystalline solids, it is necessary to determine if both the calculations based upon the dislocation model describe the gross yielding behavior of such materials, and if the model of dislocation interactions with second-phase particles utilized is consistent with observations of the deformation process. In this section, experimental data indicative of both gross yielding behavior and dislocation motion in two-phase materials, are presented in terms of the proposed theory. Since there are surprisingly few data available in which both the microstructure and yielding behavior are reported, this treatment can only be indicative of the apparent validity of the proposed theory.

1) Gross Yielding Behavior. Roberts, Carruthers and Averbach¹¹ determined the lower yield strength of several hypoeutectoid, eutectoid, and hypereutectoid steels, some of them with a pearlitic, others with a spheroidized structure. For this same series of steels, the authors optically determined the mean spacing between carbide particles or pearlite patches. Lenel, Ansell and Nelson¹² determined, by quantitative electron microscopy, the average spacing between the plate-like oxide particles, for a series of aluminum-aluminum oxide SAP-Type alloys. For these same alloys, Lenel, Backensto and Rose¹³ determined the 0.2% offset yield stress. The critical resolved shear stress of a series of overaged high-purity aluminum-copper alloys and the spacing between the dispersed second-phase particles in these alloys was determined by Dew-Hughes and Robertson.¹⁴

The two-phase materials utilized in each of these investigations are representative of three distinctly different methods of producing a dispersed phase distribution in a matrix material: eutectoid decomposition, powder metallurgy, and precipitation from solid solution. The dispersed particle size in each of these two-phase materials was relatively large; therefore the yield strength behavior predicted by equation (6a), in which the yield strength varies as the reciprocal square root of the dispersed phase spacing, should describe these data. A least squares analysis of these data shows that the yield strengths for each of these alloys varied as the reciprocal square root of the dispersed phase spacing. In addition, the observed yield strengths in each case were roughly the same as calculated from equation (6a).

In an investigation of the yielding behavior of alloys consisting of very fine spherical particles of iron dispersed in a mercury matrix, Meiklejohn and Skoda¹⁵ found for a series of these alloys which contained dispersed phase particles whose diameters ranged from 50Å to 770Å that the offset yield stress could be described by two empirically determined equations. These equations are identical to equations (6a) and (8) except for the addition of a stress constant corresponding to the determination of the offset yield stress rather than the type of yield stress predicted from the theoretical equations.

Ashbey and Smith¹⁶ determined the yield strength and spacing between dispersed oxide particles for a series of internally oxidized copper alloys.

They found that the yield strength varied as the reciprocal of the dispersed phase spacing. This is the behavior predicted by equation (6b) for a series of alloys such as these, where in each of the samples the dispersed particle diameter is of constant size and is less than $2\mu b/\sigma_{y,s}$.

The temperature dependence of the proportional limit of two aluminum-aluminum oxide SAP-Type alloys was determined by Lenel, Ansell and Bosch¹⁷ over the temperature range from 0.1 to 0.87 homologous temperature (90 to 773°K). These data indicated that the temperature dependence of the proportional limit was reasonably described by the square root of the temperature dependence of the product of the matrix and dispersed phase moduli as predicted by equation (6a).

The variation in yield strength as a function of the structural changes which occur during the aging treatment of precipitation hardened alloys has been extensively determined qualitatively.¹⁸ Figure 4 is a schematic plot of the yield strength variation versus aging time which is typical of that observed for precipitation hardened alloys. The yield strength prior to the aging heat treatment is that of the supersaturated solid solution. As aging progresses, the volume fraction of the second phase precipitate increases. Since the particle size of the precipitate is very small, the yield strength increases as predicted by equation (8); i.e., the yield strength is approximately proportional to the cube root of the volume fraction of the precipitate phase. If metastable, intermediate zones or phases are formed during the precipitation, this is reflected in the yield strength due to the variation in shear modulus associated with these precipitated phases.

At some point in the aging process, the equilibrium phase will replace any intermediate zones or phases that may have formed. From this time on the shear modulus of the precipitate remains constant and exerts no further variation on yield strength. The precipitate particles continue to coarsen as aging progresses. After all the second phase is rejected from solid solution, the only effect of aging is to coarsen the precipitate particles. The yield strength of the alloy remains constant during this process until the precipitate particle diameter is greater than $2\mu b/\sigma_{y,s}$. Until this time the yield strength is only sensitive to the volume fraction of the second phase and not to the interparticle spacing. As aging continues beyond this stage, the yield strength falls off, since the interparticle spacing increases with increased particle coarseness. Here the yield strength is given by equation (6a).

11) Dislocation Interactions with Second Phase Particles. The interaction of dislocations with dispersed oxide particles in recrystallized aluminum-aluminum oxide SAP-Type alloys has been extensively investigated by Goodrich¹⁹, utilizing transmission electron microscopy. This investigation has demonstrated three factors which are relevant toward consideration of the consistency of the theoretical treatment of the yielding behavior of two-phase materials with the observed dislocation motion in these materials.

Two of these factors are intimately connected with the validity of interpretation of transmission electron micrographs as regards the interaction of dislocations with dispersed particles during deformation of

two-phase solids. First, the dislocation configuration, upon which the theoretical model for the yielding behavior is based, is unstable and will relax if stress is removed from the two-phase system. Conventionally, the thin foils which are viewed by transmission electron microscopy are unstressed and therefore relaxed. If a bulk material is deformed, then thinned and examined in the electron microscope, the observed dislocation configuration may be totally different from the bulk dislocation configuration. This relaxation of structure is clearly demonstrated in the sequence of transmission electron micrographs shown in Figure 5. A dislocation loop surrounds a dispersed aluminum oxide particle in the first micrograph in the sequence. This configuration is consistent with the dislocation model utilized in the theoretical treatment. As shown in the rest of the sequence, this loop is unstable in the absence of an applied stress, and expands until it reaches the surface of the foil. At this time, only two dislocation segments running from one surface of the foil to the other remain. These move, leaving only the slip traces on the foil surface as evidence of the presence of the original dislocation loop. Even if the foil is stressed during observation, the nature of the dislocation particle interaction may be different in the foil as compared to the interaction behavior in bulk materials.

Figure 7, a sequence of transmission electron micrographs, shows the interaction of a moving dislocation with a group of dispersed aluminum oxide particles. A dislocation is shown moving through the foil. The edge component of the dislocation loop is blocked from further motion by the dispersed particles. The dislocation attempts to bypass the particles by bowing past them. As shown in the other micrographs of the sequence, instead of completing the bowing process, leaving residual dislocation loops about the particles as would be the case in bulk samples, the dislocation intersects the foil surface leaving a dislocation segment extending from the foil surface, around the particle, and reemerging from the foil surface. This interaction is shown schematically in Figure 8. This observation is interpreted as confirmation of the formation of residual loops about dispersed particles in bulk materials as a result of dislocations bowing between particles.

The third type of dislocation-particle interaction observed in this study which is relevant to the yielding treatment, is shown in the sequence of electron micrographs in Figure 6. In the first micrograph of the sequence, a dislocation has moved against a very small dispersed aluminum oxide particle. As shown in the second micrograph, the radius of curvature of the dislocation decreased, and the dislocation at this point cut through the particle. The shear stress on the particle due to the radius of curvature of the dislocation as calculated using equation (2b) is equal to the fracture strength of the particle calculated using equation (5).

It should be noted that except for the use of sequential photography, it would be all but impossible to obtain a meaningful interpretation of these dislocation-particle interactions.

2. Work Hardening.

The treatment of work hardening in a quantitative manner is an

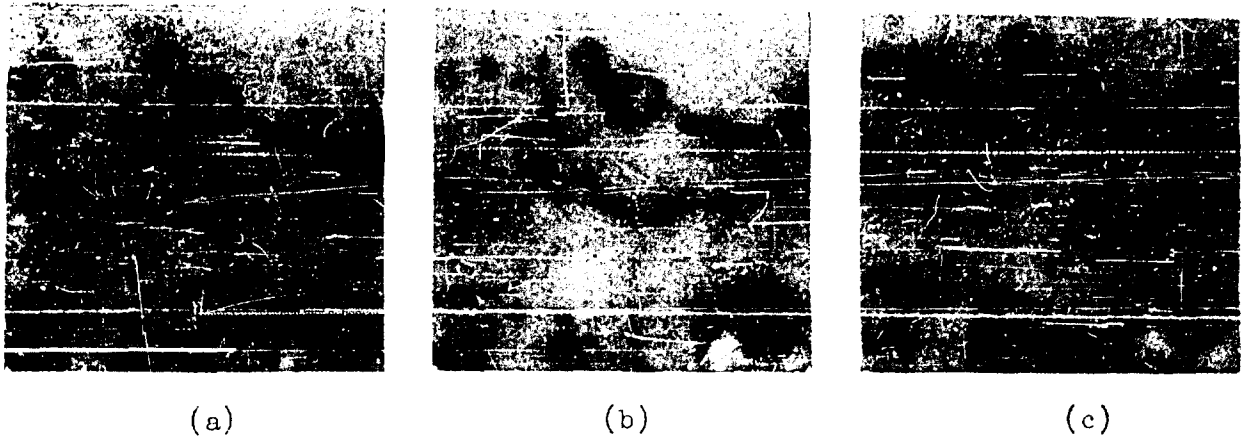


Figure 5: Sequence of dislocations relaxing away from dispersed-phase particle; 15 seconds between each micrograph.

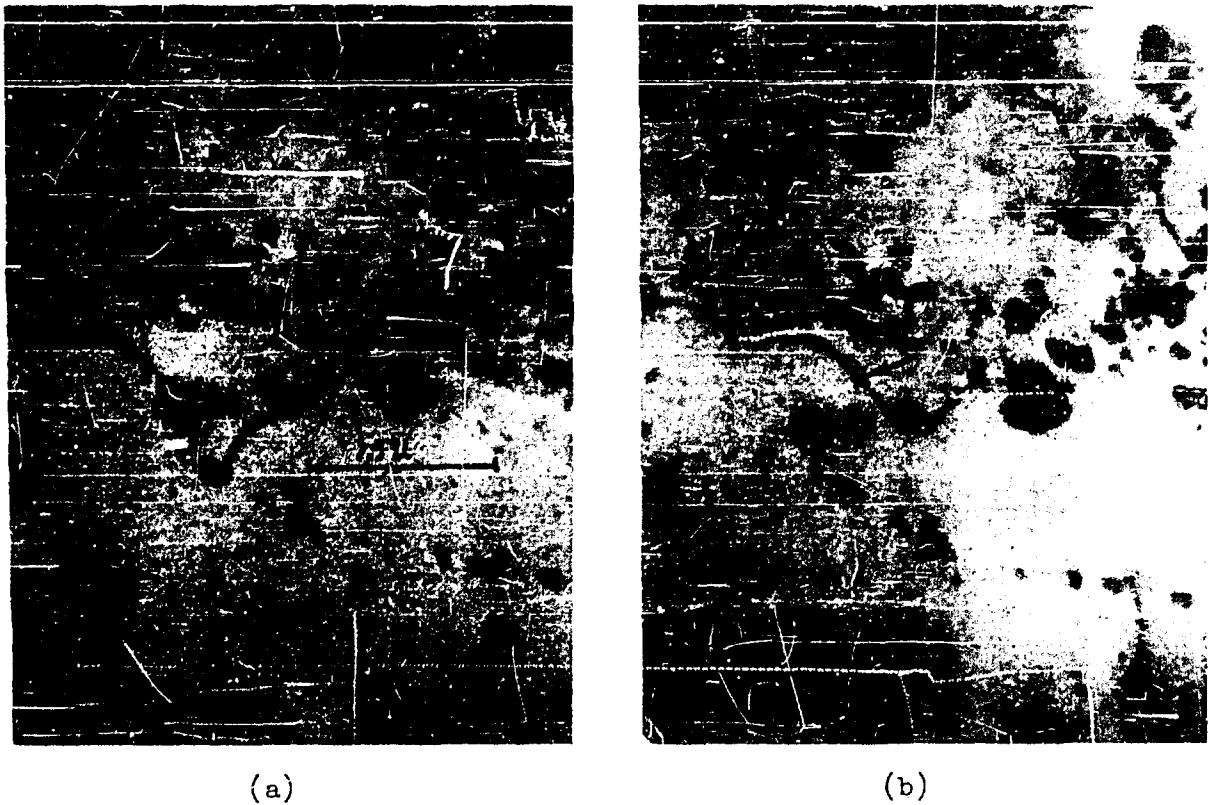
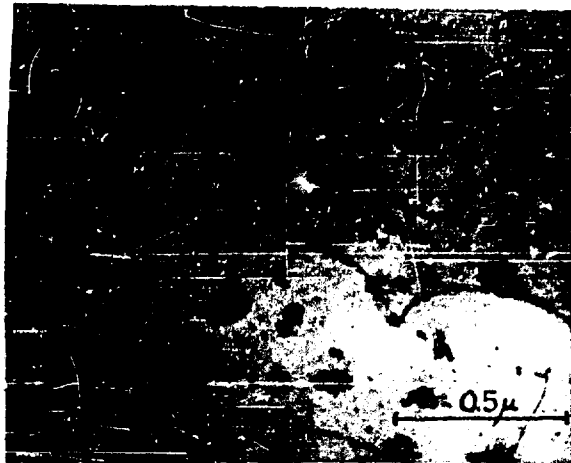


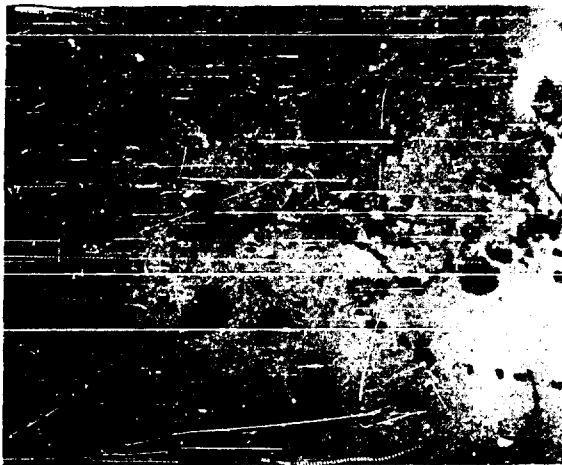
Figure 6: Sequence of dislocation cutting dispersed-phase particle; 15 seconds between each micrograph. Arrow points to jog.



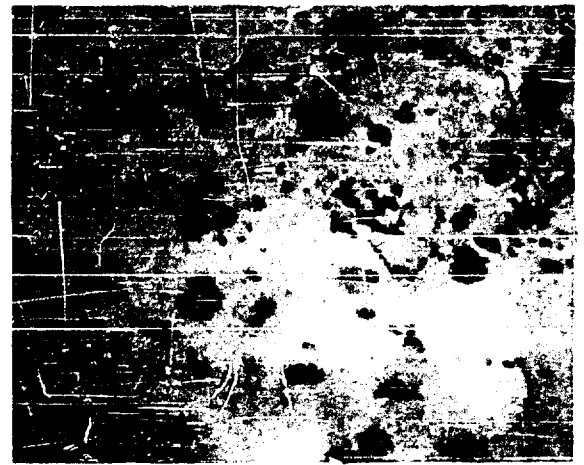
(a)



(b)



(c)



(d)

Figure 7: Sequence showing a dislocation looping about particle to emerge from foil interface; 15 seconds between each micrograph

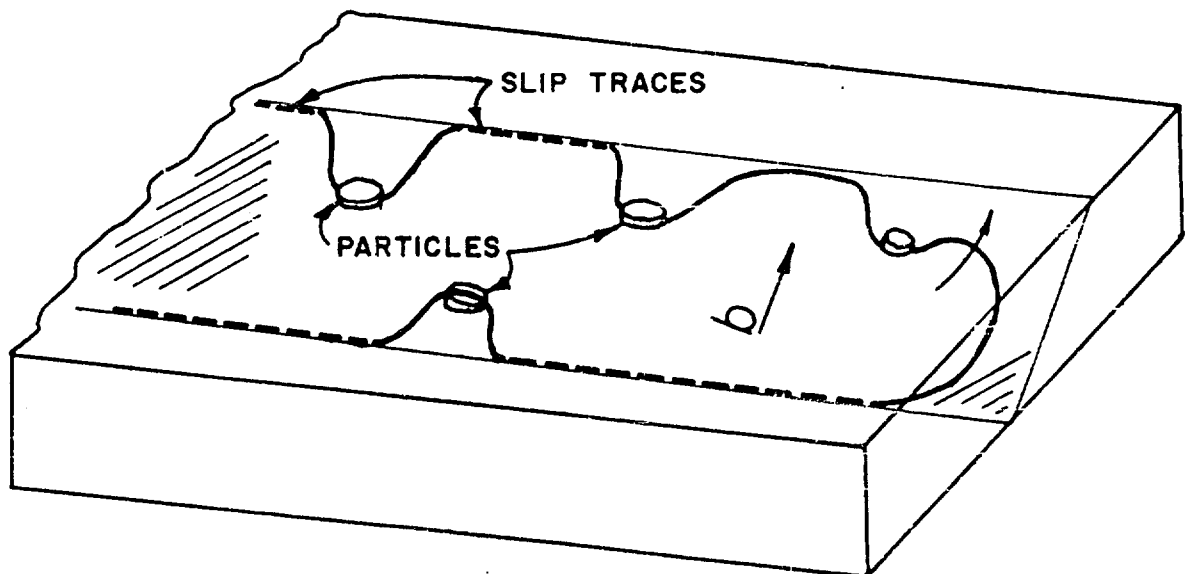


Figure 8: Schematic illustration of process shown in Figure 7.

extremely difficult task. Even in single-phase alloys, no unambiguous quantitative treatment of work hardening has yet been proposed. Hence, in this section a qualitative picture of work hardening in dispersion-strengthened alloys will be presented.

In single phase materials, Wilsdorf²⁰ has proposed that work hardening is due in large part to the formation of dislocation loops left as debris in slip planes by jogs on moving screw dislocations. These then mushroom their effect on work hardening by their interaction with successive dislocations eventually leading to dislocation tangle formation and the rapid buildup of substructure.

Goodrich has observed, utilizing transmission electron microscopy, that in the deformation of aluminum-aluminum oxide SAP-Type alloys, a similar though accelerated work hardening process occurs. The discussion which follows was developed jointly between Mr. Goodrich and the author. In addition to the jog formation mechanisms which have been observed in single-phase materials, in two-phase materials dislocation jogs are found when dislocations cut through the dispersed phase particles. This jog formation, due to cutting of the dispersed particles, is shown in the sequence of electron micrographs in Figure 6. This jog formation can be explained by the following argument. It is unlikely that the stress on the moving dislocation is a simple shear stress parallel to the active slip plane. Rather, one would expect that there is a non-vanishing component of stress normal to the dislocation slip plane which would act as a driving force for dislocation climb. Although at room temperature one ordinarily would not consider the possibility of dislocation climb in aluminum, climb over short distances is possible for the length of the dislocation line which is cutting the dispersed particle. During the cutting process, the fracture of the second-phase particle creates essentially a free surface providing an excellent source or sink of vacancies. In this region, therefore, the dislocation could climb, producing a superjog. Although the jog lies on an edge segment of dislocation lines, this segment may bear little relation to the original line orientation due to bowing during the cutting process. Since this process occurs frequently during deformation of two-phase materials moving dislocations contain a large density of jogs. This accelerated jog formation produces a dislocation configuration which, following Wilsdorf, leads to extensive tangle formation.

Concurrent to the accelerated tangle formation, the tangles intertwine with some particular configurations of dispersed particles, producing extensive volumes of the two-phase materials which contain such heavy substructure that they are essentially removed from the deformation process. Succeeding dislocation movement appears confined to relatively substructure-free volumes of the crystal. This restriction to the volume of deforming material occurs rapidly, leads to rapid work hardening, and becomes particularly important in the consideration of processes where the total deformation volume becomes important; e.g., fracture and creep.

3. Creep Behavior

Creep is the extension of crystals under constant stress at a constant temperature. Creep behavior has been described rheologically for many years.

Not all the different modes of creep which have been observed can be readily explained on the basis of a dislocation model. However, one type of creep lends itself well to such a treatment. This is steady-state creep; i.e., creep at a constant rate, at temperatures above one-half of the absolute melting temperature.

In order to treat steady-state creep, models must be set up to describe both the metallurgical structure and the dislocation configuration in the alloy and the assumption be made that both structure and configuration remain constant. The rate is then evaluated by calculating the density of dislocations moving in the crystal and their rate of motion. Two creep theories have been developed by Ansell and Weertman²¹ for dispersion-strengthened alloys. The first theory should be applicable to alloys in which the ratio of grain boundary area to volume of the alloy is small. Ansell and Weertman base their theory for the creep of these coarse-grained alloys on a model for creep essentially due to Mott and adopted by Weertman.²² According to this model, dislocation loops are created at sources under the action of an applied stress. The loops expand to some maximum radius at which point they are annihilated by climbing to dislocations of opposite sign on neighboring slip planes. Just as fast as loops are destroyed, new loops are created at the sources and steady-state creep is produced. For single-phase material the rate-controlling process for creep can be either the climb of dislocations²³ or the viscous motion of a dislocation by some microcreep mechanism.²⁴ For coarse-grained dispersion-strengthened alloys it is reasonable to assume, as suggested by Schoeck²⁵ that the rate-controlling process for steady-state creep is the climb of dislocations over the second-phase particles.

Ansell and Weertman's second creep theory was developed to account for the creep behavior of fine-grained dispersion-strengthened alloys. In this theory, it is postulated that the rate of dislocation nucleation from grain boundaries is the rate-controlling process for steady-state creep in these fine-grained dispersion-strengthened alloys.

In the following sections, each of the two theories is presented:

a) Steady-State Creep Defined by Dislocation Climb

In order to calculate steady-state creep rates based on dislocation climb, somewhat different models have to be adopted for a low stress region in which the stress is insufficient to bow dislocation loops about the particles and for a high stress region, in which the stress will cause the dislocations to bow between the dispersed-phase particles, leaving residual loops surrounding each particle.

For both of these models, assumptions must be made concerning the origin of the dislocations in the dispersion-strengthened matrix and the fractional volume of the matrix which can participate in the deformation process. The density of dislocation sources in the two-phase materials should be approximately the same as in the single-phase crystalline solid. However, since it was shown in the section on work hardening that two-phase materials have much less volume of material which can continue to deform

as compared with single-phase crystalline solids, it is not as easy to determine the fractional volume of matrix which can participate in the creep process. It is assumed, therefore, that the fractional volume of deformable matrix is some fraction, α , of the deforming volume of a single-phase material. Although at this time it is not possible to calculate a value for this fraction, α , it should be a constant for two-phase crystalline solids which have equivalent microstructures and deformation history. For this reason, the theoretical calculations made to predict the steady-state creep behavior of two-phase crystalline solids can only predict the maximum value of the absolute value of the observed creep rates. The theory should, however, quantitatively describe the effects of stress, temperature, and microstructure upon the observed creep rate.

1) Theory at Low Stresses. The creep rate in this situation may be calculated in the following manner. The creep rate is equal to the product of the fractional volume of deforming material, the number of dislocation sources per unit volume giving off dislocation loops, the plastic strain produced by one dislocation loop upon expansion to its maximum radius, and the rate of production of dislocation loops at any one source. The creep rate, $\dot{\epsilon}$, is therefore equal to:

$$\dot{\epsilon} = \alpha M \pi \bar{r}^2 b R \quad (9)$$

where α is the fractional deformable volume, M is the density of dislocation sources, \bar{r} is the maximum radius, b is the length of the Burgers vector of a dislocation, and R is the rate of creation of dislocations at one source.

The maximum radius \bar{r} can be calculated from the following argument.²³ The probability must be essentially one that at the maximum radius \bar{r} a dislocation loop is blocked from further expansion by dislocations on neighboring slip planes. Consider a pill box of radius \bar{r} and height h . Let one dislocation source be situated at the center of this pill box. There must be three other dislocation sources in the box, since it takes at least three other sources to block a dislocation loop.²⁶ These conditions mean that the value of \bar{r} must be such that

$$2 M \pi \bar{r}^2 h \approx 3 \quad (10)$$

or

$$\bar{r} \approx \sqrt{\frac{3}{2 M \pi h}} \quad (11)$$

where h is the distance climbed by a dislocation in order to annihilate a dislocation on a neighboring slip plane. In the calculation of the steady-state creep rate of a single-phase alloy, the distance h is a function of stress.²³ In the present problem the distance of climb around particles is fixed by the geometry of the dispersed-phase (distances of the order of a micron), and is usually greater than the stress-dependent values of h for single-phase alloys. Thus it is reasonable in the present calculations to take a stress-independent value of h equal to the dimensions of the particles, d .

Consider next the term R , the rate of creation of dislocation loops, which appears in equation (9). This rate is equal to the rate at which dislocations surmount the dispersed-phase particles. This is equal to the height of climb divided into the velocity of climb:

$$R = v/d \quad (12)$$

This velocity of climb is controlled by the diffusion of vacancies or interstitials. Weertman²² calculated the velocity of climb for a dislocation which could maintain an equilibrium concentration of vacancies in its vicinity. This velocity was:

$$v \approx \sigma b^2 D / kT \quad (13)$$

where σ is the stress, D is the coefficient of self-diffusion, k is Boltzmann's constant, and T is absolute temperature. The equation is valid for an edge dislocation which is climbing by itself some distance away from other dislocations.

Combining equations (9), (11), and (13), gives for the creep rate:

$$K = \alpha \pi \sigma b^3 D / 2 kT d^2 \quad (14)$$

(For unresolved stress and strain rates, the right-hand side of this equation should be divided by $2\sqrt{2}$)

ii) Theory at High Stresses. Now an expression for the creep rate will be developed for stresses great enough for dislocations to be forced past the particles by bowing about the particles, leaving residual dislocation loops surrounding and piled up against each particle. The rate-controlling process for steady-state creep now is the climb of the residual dislocation loops around the particles. The climb of these loops will be governed by the diffusion of vacancies away from or toward the dislocation loop. Since the interface between the metal matrix and the included particle should be a good source or sink of vacancies, the vacancy flow will probably be between this interface and the dislocation lines.

The rate at which the residual dislocation loops climb around the particles and become annihilated may be estimated. The loops are forced to climb around the particles because of the interaction forces of the dislocations piled up against the particles. The number n piled up in the distance λ , the dispersion spacing, is:

$$n \approx 2\sigma \lambda / \mu b \quad (15)$$

The distance a residual dislocation loop must climb, λ , before another loop can be pinched off about the particle is of the order:

$$\lambda \approx \mu b / n \sigma \approx \mu^2 b^2 / 2 \sigma^2 \lambda \quad (16)$$

The rate of climb of the dislocation loop is given by equation (13) with the stress replaced by the concentrated stress $n \sigma$ or:

$$v = 2 \sigma^2 b \lambda D / \mu kT \quad (17)$$

R , the rate of dislocation nucleation, is equal to the dislocation velocity v divided by the height of the climb, λ . Combining equations (16) and (17) yields the expression:

$$R = 4 \sigma^4 \lambda^2 D / b \mu^3 kT \quad (18)$$

Using the same argument for the dislocation source density as related to the maximum radius of expansion of dislocation loops as for the low stress case, equations (9), (11) and (18) are combined. This gives for the creep rate:

$$K = \alpha 2 \pi \sigma^4 \lambda^2 D / d \mu^3 kT \quad (19)$$

which is valid up to stresses where $n \sigma b^3 / kT$ becomes greater than one. If unresolved stresses and strain rates are used, the right-hand side of

the equation should be divided by $16\sqrt{2}$.

At stresses great enough that $\frac{n\gamma b^3}{kT}$ is greater than one, the velocity is no longer given by equation (17) but is now²²

$$v = (D/2b) \exp(n\sigma b^3/kT) \quad (20)$$

The creep rate then becomes

$$\dot{\epsilon} = (\alpha \pi \sigma^2 \lambda D / \mu^2 b^2 d) \exp(2\sigma^2 \lambda b^2 / \mu kT) \quad (21)$$

One must assume, of course, in the application of equation (21) that the included particles are strong enough to withstand the stresses exerted by the dislocations piled up against them. In the stress range where equation (21) is valid, these stresses are very large and the particles may fracture or plastically deform, giving rise to yielding of the alloy. In this case, equation (21) merely sets a lower limit to the creep rate.

b) Steady-State Creep Defined by Dislocation Generation from Grain Boundaries.

In cases where the slip length and/or dislocation mobility is severely restricted as compared with the rate of individual dislocation generation from a large number of dislocation sources, the rate-controlling mechanism for steady-state creep behavior may be a function of the rate of dislocation generation. The occurrence of this apparently anomalous process, in which the faster of two presumably consecutive processes becomes the rate-controlling process for steady-state creep behavior, is simply explained. Conventionally, one considers a system containing a constant number of operating dislocation sources. The rate of dislocation generation from these sources is controlled by the movement of previously generated dislocations away from the source, reducing the back stress on the dislocation source, allowing another dislocation to be produced. If, however, grain boundaries are the primary sources for dislocations in the material, and the grain size is very small; e.g., 5 microns in diameter, there is an extremely large number of possible sources available, only a few of which are operating to generate dislocations at any one time. If the mobility of dislocations moving from any one source is severely limited, during the period of time that the interaction or back stress of the dislocations prevents this source from generating another dislocation, some other source may become operative. Since in a fine-grained alloy there are so many available sources, one can have each source become essentially blocked after generating one dislocation and creep deformation would still continue. The creep rate, in this case, is controlled by the rate at which new sources on the grain boundary become operative. This combination of restricted dislocation mobility with a large number of available dislocation sources, should be present in a fine-grained, dispersion-strengthened alloy.

The energy required to free a dislocation from a boundary is undoubtedly stress-dependent and decreases with decreasing stress.⁵ Let it be written as $Q(\sigma)$. Then in any narrow stress range about any particular stress, σ_0 , the energy for this process can be written as:

$$Q(\sigma) = Q(\sigma_0) + \frac{dQ}{d\sigma} (\sigma - \sigma_0) \quad (22)$$

Therefore, the rate of dislocation generation, and hence the creep rate, K , can be described by an equation of the form:

$$K = A \exp(Q/kT) \exp(B\sigma/kT) \quad (23)$$

where A is a constant, Q is equal to $Q(\sigma_0) - (dQ/d\sigma)\sigma_0$ and B equals $-dQ/d\sigma$. In order to have a measurable creep rate, a stress must be applied which is sufficient to reduce Q to such a value that equation (23) will predict creep rates larger than the test sensitivity.

c) Alloy Design Based Upon Steady-State Creep Calculations.

The design of two-phase materials as regards steady-state creep behavior is discussed on the basis of the preceding calculations. Because these calculations are only applicable for levels of applied stress below the yield stress, in general the aspects of alloy design for high yield strength are also applicable to the design of two-phase materials for creep resistance.

1) Materials Selection. The coefficient of self-diffusion of the matrix is the only property of either the matrix or of the dispersed-phase which substantially affects the steady-state creep rate of two-phase materials at all stress levels. As shown in equations (14), (19), and (21), the steady-state creep rate, when dislocation-climb is rate controlling, is proportional to the coefficient of self-diffusion in the matrix. If possible, therefore, a matrix material should be chosen which has a small coefficient of self-diffusion.

At high stresses, the steady-state creep rate is inversely proportional to the cube of the matrix shear modulus. In addition, the stress which delineates the change in creep behavior from low stress, equation (14) to high stress, equation (19), behavior is directly proportional to the shear modulus of the matrix. Since this stress indicates the transition between a steady-state creep rate which is proportional to the applied stress to one which is proportional to the fourth power of the applied stress, the matrix material should have a high shear modulus.

It is interesting to contrast the materials selection for increased creep resistance with the materials selection for increased yield strength. For creep resistance the choice of matrix material is of primary importance. For increased yield strength, if the dispersed-phase is sufficiently fine, only the selection of the dispersed-phase material is important.

ii) Dispersed-Phase Morphology. Inspection of equations (14) and (19) indicates that the steady-state creep rate is independent of interparticle spacing at low stress levels, while at high stresses, the creep rate is inversely proportional to the square of the dispersion spacing. In addition, the stress which delineates low and high stress behavior is inversely proportional to the dispersion spacing. In fabricating a two-phase material for greatest creep resistance, the mean free path between dispersed phase particles should, therefore, be as small as possible.

For low stress levels, the creep rate is inversely proportional to the square of the height of the particle as shown by equation (14). At

high stresses, however, inspection of equation (19) shows that the creep rate is inversely proportional to the height of the particle. In considering the shape of dispersed-phase particles when designing alloys for increased creep resistance, the combination of fine spacing and large particle height dictates the preference for plate-shaped particles.

iii) Matrix Grain Size. As indicated by equation (25), if the matrix grain size is extremely fine, the steady-state creep rate will not be governed by dislocation climb, but rather be controlled by the rate of dislocation generation from grain boundaries. This would produce an increased creep rate as compared to the same two-phase material where dislocation climb was rate-controlling. For increased creep resistance, the grain size of the matrix should be coarse.

iv) Service Temperature. The effect of temperature upon the steady-state creep behavior of two-phase materials can be separated into two areas, structural stability and temperature sensitive parameters in the creep equations.

The creep equations have been derived based upon a discrete microstructural configuration of dispersed-phase particles in a crystalline matrix. Any change in the dispersion morphology will therefore change the creep behavior. The effect of temperature upon microstructural configuration is, of course, to reduce the overall system energy by spheroidizing and coarsening the dispersed particles and attendantly increasing the interparticle spacing. These processes all act to reduce creep resistance. The problem of providing structural stability in two-phase materials has been discussed previously, although perhaps not very satisfactorily, in this paper. Of all the aspects of alloy design for creep resistance, the structural stability is probably the most important, and the least well understood.

If the structure is completely stable, the variation of creep rate with temperature is governed primarily by the activation energy for self-diffusion in the alloys where dislocation climb is rate-controlling and by the stress dependent activation energy for dislocation generation from grain boundaries where dislocation generation is the rate-controlling process for steady-state creep. Additionally, when dislocation climb is the rate-controlling process for creep, the creep rate is inversely proportional to absolute temperature, and at high stress levels the creep rate is inversely proportional to the cube of the stress-dependence of the matrix shear modulus.

d) Consistency of Steady-State Creep Behavior with Experimental Observations.

In order to consider the validity of this proposed treatment of the creep behavior of two-phase crystalline solids, it would be desirable to determine both if the calculations based upon the dislocation models describe the observed creep behavior of such materials, and if the dislocation models utilized are consistent with direct observations of the deformation process. Unfortunately, there is little data available which

describes the steady-state creep behavior of these materials, and no data which concerns the nature of dislocation motion in two-phase materials during the creep process. In this section, therefore, some experimental steady-state creep data are presented in terms of the theory in order to indicate the apparent validity of the proposed theory.

1) Data for Alloys where Dislocation Climb is the Rate-Controlling Process for Steady-State Creep. Steady-state creep data for two coarse-grained, recrystallized, aluminum-aluminum oxide SAP-Type alloys have been obtained by Ansell and Lenel.^{27,28} These alloys, designated AT-400 and RP 15-30, were fabricated by compacting, hot pressing, and then hot extruding two different grades of atomized aluminum powder. After this initial fabrication process, the alloys were heavily cold worked by wire drawing and then annealed. These recrystallized alloys, consisted of a fine dispersion of aluminum oxide platelets in a relatively coarse grained (several millimeters in diameter)²¹ aluminum matrix. The dispersion spacing was approximately 1 micron for the AT-400 alloy, and 6 microns for the RP 15-30 alloy.¹²

Samples of these recrystallized alloys were creep tested at various stresses, and temperatures. In Figure 9, the steady-state creep rates for the two alloys at 500°C are shown on a logarithmic scale as a function of stress. In addition, the creep rates predicted by equations (14) and (19) for these alloys, assuming $\alpha = 1$, at 500°C, and the creep rates of high purity aluminum at 483°C, are also shown. From these experimental data and the calculated creep rates, several factors became apparent. First, the volume fraction of deforming material, α , is quite low as indicated by the difference in rates predicted theoretically, assuming $\alpha = 1$; i.e., equivalent to single-phase materials, as compared with the observed creep rates. Second, the steady-state creep rates of these alloys at high stresses vary, as predicted, as the fourth power of the applied stress. Third, the creep rates in this stress range are proportional to the dispersion spacing. The creep rate of the RP 15-30 alloy is about 32 times faster than the rate of the AT-400 alloy at the same stress, while their respective dispersion spacings are at a ratio of 6 to 1.

In order to determine the effect of temperature upon the creep behavior, two methods were utilized. First, the activation energy for steady-state creep was determined experimentally by conducting creep tests on the AT-400 alloy in which the stress was held constant and the test temperature suddenly changed. Using equation (19), a value for the activation energy, Q , of 37,000 cal/mole was determined from the creep rates at the two temperatures. This value of activation energy for creep is in good agreement with the activation energy for self-diffusion in aluminum, indicating that dislocation climb is the rate-controlling process for steady-state creep in this alloy. Second, utilizing equation (19) and the experimentally determined value of the activation energy, the creep data obtained at several different temperatures, over a wide range of stress, was normalized to a single test temperature. A plot of this normalized data provided a continuous relation of creep rate as a function of stress, further indication of the apparent validity of the theoretical treatment.

Lenel⁹ has determined the steady-state creep behavior of a series of

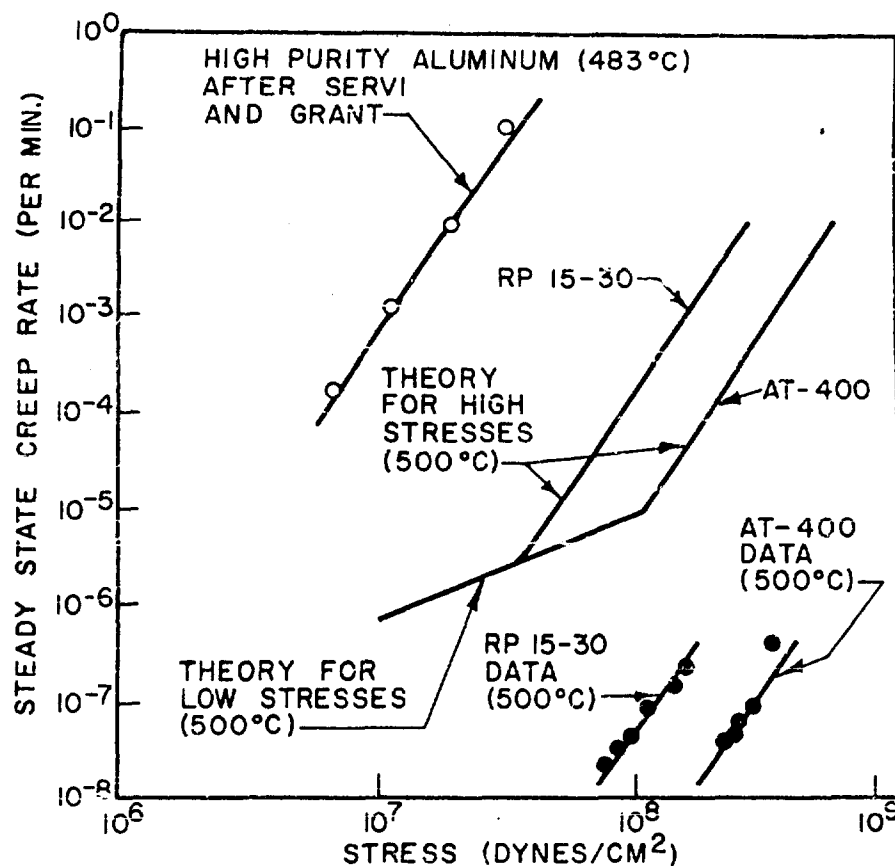


Figure 9: Steady-state creep rate is plotted as function of the applied stress for high purity aluminum and two aluminum-aluminum oxide SAP-Type alloys. Theoretical curves are shown assuming $\alpha = 1$



(a)



(b)

Figure 10: Electron fractographs of the fracture surfaces of a) commercial purity aluminum and b) aluminum-aluminum oxide SAP-Type alloys.

dispersion-strengthened lead alloys over a wide range of stress (200 to 2000 psi). His analysis of these data indicated that the creep rate of these alloys at low stresses was proportional to the applied stress, while at high stresses it was proportional to the fourth power of the stress.

ii) Data for Alloys where Dislocation Generation From Grain Boundaries is the Rate-Controlling Process for Steady-State Creep. Steady-state creep data has been obtained for two fine-grained as-extruded aluminum-alumina oxide SAP-Type alloys by Ansell and Weertman²¹, and Achter and Lloyd.²⁹ These alloys, MD-2100 and M-257 in the as-extruded condition, have needle-like grains, about five microns in diameter, but many microns long. Both have an average dispersed-particle spacing of approximately 0.5 microns. M-257 is a commercial grade of Aluminum Powder Metallurgy Product.

The steady-state creep rates of the two fine-grained alloys, when measured at a single temperature, followed an equation of the type:

$$K = A \exp(B\sigma/kT) \quad (24)$$

where A and B are constants.

The data from several test temperatures could be normalized to a single test temperature, utilizing equation (23). Thus these data are in qualitative agreement with the proposed theory.

4. Fracture Mode.

In general, when a two-phase aggregate fractures, the separation mode is a complex process which can be categorized in simple terms only under certain conditions. In spite of this problem, however, it is possible to delineate the effects of the dispersed-phase upon the fracture process in a qualitative way.

The presence of a dispersed-phase has a direct effect on the mode of fracture and inherent ductility of dispersion-strengthened alloys.^{30,31} In a metal matrix the dispersed-phase particles provide sites of high local stress concentration, restrict dislocation mobility and reduce rapid work hardening. The combination of local stress concentrations with restricted dislocation mobility can provide conditions where cleavage cracks can be nucleated even in a fcc metal matrix. This behavior is in direct contrast to single-phase fcc crystals where cleavage cracks normally cannot be nucleated, either because dislocation barriers are too weak, or because dislocations have the ability to circumvent barriers by cross slip. In addition, the high dislocation mobility in these single-phase crystals allows stress relaxation to occur at the tips of rapidly moving cracks introduced by other means.

In a relatively ductile metal matrix the dispersed-phase, therefore, generally acts to reduce ductility because of the increased tendency towards crack nucleation and growth coupled with rapid work hardening. In Figure 10 electron micrographs of the fracture surfaces of pure aluminum and aluminum containing a fine dispersion of aluminum oxide are shown.³² Both samples were broken in impact at room temperature. The fracture surface of the aluminum sample is characteristic of a ductile failure, while that of the dispersion-strengthened alloy shows evidence of crack nucleation and generation.

In a relatively brittle metal matrix where the dislocation mobility is restricted even without the presence of a dispersed second phase, the addition of a dispersed-phase can act to increase ductility. This apparent anomaly arises from the following argument:²¹ In addition to the effects of a dispersed-phase discussed in connection with a ductile metal matrix in brittle materials where crack generation is relatively easy, the dispersed-phase particles serve to: a) provide sites where cleavage cracks may open ahead of an advancing crack front; b) dissipate the stress concentration which would otherwise exist at the crack front; and c) alter the local effective state of stress from plane strain to one of plane stress in the neighborhood of the crack tip. Provided that the temperature is not too low, the average crack velocity is thereby reduced and the average work done per unit area of fracture surface is increased.

Variations in the effect of the dispersed-phase upon fracture mode may be achieved by changes in dispersed particle morphology and in the character of the matrix-dispersed phase interface. The interesting result of this argument concerning fracture mode is that a dispersion-strengthened alloy may be more or less ductile than its metal matrix, depending primarily on the inherent ductility of the matrix alone.

Discussion

In the preceding sections, several of the strength properties of dispersion-strengthened alloys (i.e., yielding behavior and steady-state creep) have been handled in a rather fundamental way with a fair degree of success. The other properties discussed have been handled in a rather qualitative manner because of the difficulty of considering them in terms of a unique dislocation or metallurgical structure. In these areas, however, at least the experimental data provided sufficient insight to provide a qualitative description.

There are some properties of dispersion-strengthened alloys which at the present time defy either a fundamental or qualitative treatment. These include, among others, recovery and transient creep behavior. Since it appears pointless to present unconnected experimental data in areas where there is little understanding at this time, this treatment does not include any other mechanical properties of two-phase alloys.

Acknowledgements

The author wishes at this time to gratefully acknowledge the informative and useful discussions held with many individuals in connection with the presented material. I am indebted for the discussions with Professor F. V. Lenel, Professor J. Weertman, Dr. R. W. Guard, and Dr. T. L. Johnston. In addition, the permission of Mr. R. S. Goodrich, Jr., to allow the use of some of his interesting transmission electron microscopy observations prior to their inclusion in his doctoral dissertation is particularly acknowledged.

The work reported in this paper was supported by both the Office of Naval Research and the National Aeronautics and Space Administration. The most recent studies were carried out in the NASA Interdisciplinary Materials Research Center at Rensselaer Polytechnic Institute.

REFERENCES

1. Goetzel, C. G., J. Metals, 11, 189, 276 (1961)
2. Irrmann, R., Aluminium, 27, 29 (1951)
3. Ansell, G. S. and F. V. Lenel, Acta Met., 8, 612 (1960)
4. Ansell, G. S., Acta Met., 9, 518 (1961)
5. Cottrell, A.H., Dislocations and Plastic Flow in Crystals, Clarendon Press, Oxford (1953)
6. Kelly, A. and M.E. Fine, Acta Met., 5, 365 (1957)
7. Barrett, C.S., Acta Met., 1, 2 (1953)
8. F. W. Starratt, Dispersion Strengthened Alloys, Jn. Met., 8, 561 (1962)
9. Lenel, F.C., Powder Metallurgy, No. 10, 119 (1962)
10. Adachi, M. and N. J. Grant, Trans. AIME, 218, 881 (1960)
11. Roberts, C.S., Carruthers, R.C., and B. C. Averbach, Trans. Am. Soc. Metals, 44, 1150 (1952)
12. Lenel, F.V., Ansell, G.S. and E. C. Nelson, Trans. AIME, 209, 117 (1957)
13. Lenel, F.C., Backensto, A.G. Jr., and M. V. Rose, Trans. AIME, 209, 124 (1957)
14. Dew-Hughes, D., and W. D. Robertson, Acta Met., 8, 147 (1960)
15. Meiklejohn, W.H. and R. E. Skoda, Acta Met., 7, 675 (1959)
16. Ashbey, M.F. and G. C. Smith, Phil. Mag., 5, 298 (1960)
17. Lenel, F. V., Ansell, G.S., and R.A. Bosch, Trans. AIME, 221, 892 (1961)
18. Geisler, A.H., Phase Transformations in Solids, Wiley, New York (1951)
19. Goodrich, R.S. Jr., Private Communication of material which is to be included in Doctoral Dissertation, Rensselaer Polytechnic Institute, Troy, New York (1963)
20. Kuhlmann-Wilsdorf, D., Maddin, R., and H.G.F. Wilsdorf, Strengthening Mechanisms in Solids, Am.Soc. for Metals, Cleveland (1962)
21. Ansell, G.S. and J. Weertman, Trans. AIME, 215, 838 (1959)
22. Weertman, J., J. Appl. Phys., 26, 1213 (1955)
23. Weertman, J., J. Appl. Phys., 28, 362 (1957)
24. Weertman, J., J. Appl. Phys., 28, 1185 (1957)
25. Schoeck, G., Creep and Recovery, Am.Soc. For Metals, Cleveland (1957).
26. Friedel, J., Phil. Mag., 46, 1169 (1955)
27. Ansell, G.S. and F. V. Lenel, Trans. AIME, 221, 452 (1961)
28. Lenel, F.V. and G. S. Ansell, Proceedings First International Conference on Powder Metallurgy, Interscience, New York (1961)
29. Achter, M., and G. Lloyd, Private Communication.
30. Low, J.R., Fracture, Wiley, New York (1959)
31. Johnston, T.L., Stokes, R.J. and C. H. Li, Trans. AIME, 221, 792 (1962)
32. Ansell, G. S. and H. Kim, Powder Metallurgy, No. 10, 61 (1962)